Applied Mathematical Sciences, Vol. 14, 2020, no. 16, 781 - 800
HIKARI Ltd, www.m-hikari.com
https://doi.org/10.12988/ams.2020.914273

Synergistic Effects of Oncolytic Adenovirus and MEK Inhibitors on Glioma Treatment Dynamics: Analysis and Optimal Control

M. Kabong Nono [1*], E. B. Megam Ngouonkadi [1,2], S. Bowong [3], H. B. Fotsin [1]

[1] Unité de Recherche de Matière Condensée, d'Electronique et de Traitement du Signal (URMACETS), Department of Physics, Faculty of Sciences, University of Dschang, P.O. Box 067 Dschang, Cameroon
[2] Department of Electrical and electronics Engineering, College of Technology, University of Buea, P.O. Box 063 Buea, Cameroon
[3] Department of Mathematics and Computer Science, Faculty of Sciences, University of Douala, P.O. Box 24157 Douala, Cameroon
[*] Corresponding author

Abstract

In this paper, we investigate the dynamics and optimal control of a combination therapy model of glioma with adenoviruses and MEK inhibitors. We provide a theoretical study of the model. We derive the basic reproduction number $\mathcal{R}_0$ which determines the extinction and the persistence of adenovirus in the tumor environment. More precisely, we compute equilibria and study their stability. Based on Lyapunov theory, we show that the infection-free equilibrium is globally asymptotically stable whenever $\mathcal{R}_0 < 1$. However, if $\mathcal{R}_0 > 1$, there exist a unique uniform equilibrium which is locally asymptotically stable. The sensitivity analysis of $\mathcal{R}_0$ is performed in order to determine the impact of related parameters on therapy. Furthermore, the model can present a Hopf bifurcation. Finally, we applied the optimal control to our model and we found that, through an optimisation of a combined oncolytic virotherapy and MEK inhibitors. The obtained results furnish potentially useful information to improve treatment with this combined therapy into which biomedical benefits were included. The optimality proviso agrees that tumor load can be reduced under successive ther-

apies' infusion. At any stage, the theory is supported by numerical simulations.

Mathematics Subject Classification: 34D23, 34A34, 92C60, 49K15

Keywords: Glioma, Oncolytic Adenovirus, MEK inhibitor, Bifurcation, Optimal control

1 Introduction

Among many type of human cancers, gliomas are the most common and serious type of brain cancer arising from glial cells, which are the supportive cells for neurons, and their incidence is increasing over time [3]. They are characterized by highly proliferative growth and malignancy, which make up approximately 30% of all brain and central nervous system tumors and 80% of all malignant brain tumors. Standard radiotherapy, chemotherapy and surgery treatment have major limitations due to the cancer's genomic instability, heterogeneity, and their locations beyond the blood-brain barrier [18]. That is why, combined therapies are frequently used to extend patients survival while reducing their morbidity. Unfortunately, in many cases, the disease ends up escaping to the treatments. Moreover, chemotherapies usually have side-effects on the patient and they are not enough to control the generalized disease, especially because the cancer cells develop resistances. Despite many novel anticancer drugs are constantly sought, all these treatments procedures are ineffective since patients diagnosed with the high grade manifestation called Glioblastoma Multiforme (GBM) continue to face poor prognosis with a median survival time no longer than 15 months [22].

In the past two decade subsequent research has revealed that oncolytic viruses are an emerging therapy tool for tumors that currently lack effective treatment [28, 16]. The efficiency of this new form of treatment called virotherapy have been studied in various types of cancer, including malignant gliomas with in vitro and in vivo experiments [8]. Virotherapy of tumors has gained credence, particularly in glioma management, as these tumors are not completely resectable and tend to micro-metastasize. Major studies on virotherapy of gliomas have been conducted using various oncolytic viruses such as Measles virus, reovirus, herpes simplex viruses, adenoviruses, vesicular stomatitis virus and measles viruses to name a few [28, 23]. Adenoviral vectors have an advantage over other viral vectors in that, they are relatively non-toxic and do not integrate in the genome. In particular, many self-amplifying, or "replication-competent" adenoviral vectors with cancer-selective replication properties, also known as Conditionally Replicative Adenoviruses vectors (CRAds), exhibit strong oncolytic anti-glioma effects [26]. CRAds are adenoviruses typically

lack the EIB and/or EIA genes; these viral genes inactivate the cellular p53 and retinoblastoma (Rb) tumor suppressor genes that are frequently mutated or inactivated in human cancers. Thus CRAds will replicate in tumor cells lacking p53 and/or Rb, although other mechanisms of tumor selectivity may be operative [25]. For example, Adenovirus dl1520, also known as ONYX-015, faulty in the EIB-55KDa protein, showed significant tumor cell killing and reduction in tumor mass in preclinical experiments both in vivo and in vitro as well as in phase I clinical trial [4]. However, the lack of Coxsackievirus and Adenovirus Receptors (CAR) on surface of gliomas provides for inefficient transduction of wild-type adenoviral vectors in these tumors [11]. In fact, studies in clinical trials have shown that the entry of an adenovirus into tumor cells is, complicated by the reduction or total absence of CAR in tumor cells in general and GBMs in particular [11]. Since the CAR levels in gliomas are low [23], targeting the adenovirus to gliomas therefore remains a challenge.

Mitogen-activated protein kinase kinase (MEK, also known as MAP-kinase kinase) inhibitors have been shown to promote CAR expression, and could result in increased ONYX-015 entry into target cells [29]. This could lead to a novel combined therapeutic approach to cancer, using ONYX-015 and MEK inhibitors. However, MEK inhibitors can cause temporary cell-cycle arrest, which inhibits the life-cycle of ONYX-015. So, MEK inhibitors may limit the replication of virus. To design an effective protocol of synergetic effects of CRAds and the latter against cancer, the positive effect of MEK inhibitors should be optimally balanced with their negative effect. This complicates the dynamics of the set constituted of MEK inhibitors, viruses and tumor cells.

The dynamics of combination therapy of cancer using CRAds and MEK inhibitors has been initially introduced by Zurakowski and Wodarz [29], who proposed an ODE model to describe the effects of MEK inhibitors and viruses on tumor cells and use it to explore the reduction of the tumor size that can be achieved by the combined therapies. More recently, Baba et al. [1] analytically demonstrated the conditions that lead to optimal therapy in minimizing glioma cells proliferation using a spatiotemporal mathematical model that describes interaction between tumor cells and oncolytic viruses. They postulated that virotherapy always fails when the amount of MEK inhibitors is large. However, this model did not take into account the dynamics of CAR expression on the cells surface. Also, the virus replication in tumors as well as the lytic cycle of oncolytic virus is not well understood. In fact, the lytic activity of viral particles is an important process in oncolytic virotherapy [6, 9].

This work aims to complement and extend the aforementioned studies, by designing and analyzing a more comprehensive and realistic model for gaining insights into the combination therapy of glioma using CRAds and MEK inhibitors. The outline of the remainder of manuscript is as follows. The model is presented in section 2 with some properties of solutions. In section 3 some

important results (existence of equilibria, local stability and bifurcations) are given. Optimal control problem is formulated in section 4 to derive possible treatment strategies using Pontryagin's Maximum Principle, followed by some numerical simulations with biological implications. Concluding remark of our research are then given in section 5.

2 Mathematical model

2.1 Model formulation

Herein, we present the mathematical temporal model describing the dynamics of glioma treatment with oncolytic adenoviruses over time. The model that we use in our work is an extension of those presented in [29] and [1] with some meaningful modifications. Firstly, we assume that uninfected tumor cells grow logistically, since this growth model captures a decelerating rising rate as tumor increases in size as is observed experimentally [16]. Secondly, we consider a missing term which represents the elimination of free virus particle. In fact, as mentioned in [19], it is assumed that one virus particle infects one cell, and once a virus enters a cell, it is incapable of infecting additional cells and cease to be part of free virus population. Also, we incorporate one of the key parameter which characterize the lytic cycle within infected tumor cells namely the viral burst size, i.e the number of new viruses released from a lysis of an infected cell [9]. The model includes four variables: uninfected cancer cells, x, infected cancer cells, y, free virus particles, v and the average level of CAR molecules on the surface of the cells, w. It is given by the following set of differential equations which describes the development of these populations over time.

$$\begin{cases} \dot{x} &= r(1-u)x(1-\frac{x+y}{K}) - \frac{\beta w x v}{1+\alpha v} - \mu x, \\ \dot{y} &= \frac{\beta w x v}{1+\alpha v} - \delta(1-u)y - \mu y, \\ \dot{v} &= b\delta(1-u)y - \frac{\beta w x v}{1+\alpha v} - \gamma v, \\ \dot{w} &= \eta u(p-w) - hw. \end{cases} \tag{1}$$

In (1), different parameters have the following interpretations. The population of uninfected tumor cells replicates at a rate r which is slowed down by the intensity of MEK inhibitor captured by the parameter u through the term $(1-u)$. Furthermore, uninfected tumor cells population has a natural death rate, μ. For the first equation of system (1) to be biologically meaningful, and the whole interaction system to be mathematically tractable, we assume that $r(1-u) > \mu$ i.e $u < 1 - \mu/r$. Otherwise, the cancer cells population, x will collapse in finite time. This condition implies the assumption that, we can not apply MEK inhibitors in a dose sufficient to result elimination of cancer cells population in finite time. This condition also guaranties

the existence of a physical realistic maximum size of cancer cells population given by $K\left(1-\frac{\mu}{r(1-u)}\right)$. Thus in this work, we will consider as in [29] that $u < 1-\mu/r$. If $u = 0$, there is no drug treatment, that is no cells enter G1 arrest and there is no production of the CAR molecules. If $u = 1$, the drug has the maximum possible effect and all cells enter G1 arrest and the production of the CAR molecule is at its theoretical maximum. When the virus meets susceptible cells, infection can occur. This requires the interaction of free virus with a CAR receptor on a susceptible cell, which occurs at a rate βwxv. The infection rate is thus proportional to the average number of receptors on the cell surface, w, the concentration of free virus v, and the concentration of susceptible cells x. As the virus becomes hyper-abundant relative to the uninfected cells, multiple infections of already infected cells become more likely than infection of uninfected cells, so the infection rate saturates with v as the term $1/(1+\alpha v)$. The saturation effect accounts for the fact that the number of contacts of an individual cell reaches some maximal value as the immune system evolves to stop a virus just as the virus evolves to enter cells and replicate [29]. The infected cells can die due to two mechanisms: the natural death rate denoted by the parameter μ and the virus-induced death rate by lyses represented by parameter δ, to release b viruses per infected tumor cells. The virus-induced death rate is proportional to $(1-u)$. That is, as the activity of the inhibitor is increased, the rate of virus induced cell death declines. The reason is that, virus induced cell death requires virus production and this does not occur in the presence of the inhibitor because the cells are arrested in G1. The free viruses are eliminated at the rate γ by various causes including non specific binding and generation of defective interfering particles. We assume that CAR is produced by cells with a rate η, and production is related to inhibitor activity, u. That is, the stronger the inhibitor activity, the higher the production rate of CAR. The term $(p-w)$ represents the saturation of CAR expression. That is, the cell cannot bear an infinite number of receptors, but production declines and stops as their number on the cell surface increases. CAR is lost from the cell surface with a rate h.

The values and ranges of the parameters used in our model are given in Table 1.

2.2 Well-posedness of the model

For the model to be ecologically meaningful, it is important to prove that all the state variables are non-negative as time evolves. It is not difficult to have the following result.

Theorem 1: *The model system (1) is a dynamical system in the biological feasible compact domain* $\mathcal{D} = \left\{(x,y,v,w) \in \mathbb{R}^4_+, x+y \leq K\left(1-\frac{\mu}{r(1-u)}\right); v \leq \frac{Kb\delta}{r\gamma}\left(r(1-u)-\mu\right); w \leq \frac{\eta up}{\eta u+h}\right\}$.

Table 1: Description and values of parameters

Parameter	Description	Baseline value	Range	References
r	Tumor cell growth rate	$0.5\ day^{-1}$	$0.12 - 1.2$	[8]
K	Tumor cell carrying capacity	$2 \times 10^9\ cells$	$10^9 - 2 \times 10^9$	[16]
β	Viral infection rate	$1.2 \times 10^{-10} pfu^{-1}.day^{-1}$	$4 \times 10^{-12} - 1.26 \times 10^{-10}$	[19]
u	efficiency of MEK inhibitors	0.5	$0 - 1$	[1, 29]
α	The Reciprocal half saturation constant	$1.95 \times 10^{-10}\ cell^{-1}$	$(0 - 2) \times 10^{-10}$	[29]
μ	Natural death rate of cells	$0.1\ day^{-1}$	$0.001 - 0.3$	[7, 29]
δ	Death rate of infected cells	$0.5\ day^{-1}$	$0.5 - \frac{8}{3}$	[8, 19]
b	Burst size of infected cells	$1000\ pfu.cell^{-1}$	$0 - 1000$	[8, 19]
γ	Viral clearance rate	$24\ day^{-1}$	$0.24 - 24$	[8, 19]
η	Production rate of CAR	$0.17\ day^{-1}$	–	[29]
p	Maximum number of CAR on cell surface	2	$1 - 10$	[29]
h	Loss rate of CAR from the cell surface	$0.07\ day^{-1}$	–	[29]

3 Analysis of the model

3.1 Infection-free equilibrium (IFE) and its stability

The system has two infection-free equilibria that are given by $E_0 = (0, 0, 0, w_0)$ and $E_1 = (x_0, 0, 0, w_0)$, where $w_0 = \frac{\eta u p}{\eta u + h}$ and $x_0 = K\big(1 - \frac{\mu}{r(1-u)}\big)$.
The equilibrium E_0 represents the condition that none of the cell or virus population exist. From the Jacobian matrix at the equilibrium E_0, it is obvious that, E_0 is stable if $r(1-u) - \mu < 0$ i.e $u > 1 - \mu/r$.
This implies that the tumor could be eradicated with a sufficiently high dose of MEK inhibitors. But, this is not feasible since $u < 1 - \mu/r$ (see section 2.1).
For the equilibrium E_1, the Jacobian matrix is

$$J(E_1) = \begin{pmatrix} \frac{-r(1-u)}{K}x_0 & \frac{-r(1-u)}{K}x_0 & -\beta w_0 x_0 & 0 \\ 0 & -\delta(1-u) - \mu & \beta w_0 x_0 & 0 \\ 0 & b\delta(1-u) & -\beta w_0 x_0 - \gamma & 0 \\ 0 & 0 & 0 & -\eta u - h \end{pmatrix}$$

It is clear that $-\frac{r(1-u)x_0}{K}$ and $-(\eta u + h)$ are eigenvalues of $J(E_1)$. Thus, the local stability of E_1 is completely determined by the determinant and the trace of the following sub-matrix:

$$J_0 = \begin{pmatrix} -\delta(1-u) - \mu & \beta w_0 x_0 \\ b\delta(1-u) & -\gamma - \beta w_0 x_0 \end{pmatrix}.$$

The sub-matrix J_0 is stable if its trace is negative and its determinant is non-negative. Therefore, a sufficient condition for the equilibrium E_1 to be stable is given by $\frac{\beta w_0 x_0 b\delta(1-u)}{(\delta(1-u)+\mu)(\gamma+\beta w_0 x_0)} < 1$.

It is well known that the threshold value that determines the stability of the infection-free equilibrium is the infection basic reproduction number $\mathcal{R}_0$, which is the average number of new uninfected cancer cells infections generated by one infected cancer cell, via lysis, during virotherapy in a completely susceptible

cell population [17, 27]. Thus, the basic reproduction ratio of the model (1) is given by

$$\mathcal{R}_0 = \frac{\beta b \delta w_0 x_0 (1-u)}{(\delta(1-u)+\mu)(\gamma+\beta w_0 x_0)}. \tag{2}$$

It is clear that $\mathcal{R}_0$ is always positive when E_1 exists. Consequently, we have the following result.

Lemma 2: *The infection-free equilibrium of model system (1) is locally asymptotically stable (LAS), whenever* $\mathcal{R}_0 < 1$ *and unstable if* $\mathcal{R}_0 > 1$.

Biologically, lemma 2 means that if $\mathcal{R}_0 < 1$ the tumor can not be eradicated in the host, since the glioma cells reach their maximum value.

Now let us study the global stability of the infection-free equilibrium E_1. The strategy of proof is the use of a suitable Lyapunov function and Lasalle's invariance principle.

Proposition 3: *If* $\mathcal{R}_0 < 1$*, then the infection-free equilibrium* E_1 *is globally asymptotically stable.*

Proof: Consider the following positive definite real valued function

$$L = \delta(1-u)y + \frac{\delta(1-u)+\mu}{b}v. \tag{3}$$

Straightforward computation shows that the derivative of L with respect to t is given by $\frac{dL}{dt} = \delta(1-u)\frac{\beta w x v}{1+\alpha v} - \frac{\delta(1-u)+\mu}{b}\left[\frac{\beta w x v}{1+\alpha v} + \gamma v\right]$. Since $\frac{v}{1+\alpha v} \leq v$, $\underset{t\to\infty}{lim\,sup}(w(t)) \leq w_0$ and $\underset{t\to\infty}{lim\,sup}(x(t)) \leq x_0$, we have $\frac{dL}{dt} \leq \frac{(\delta(1-u)+\mu)(\beta w_0 x_0+\gamma)(\mathcal{R}_0-1)v}{b}$.

It follows from the above equations that $\frac{dL}{dt} \leq 0$ when $\mathcal{R}_0 < 1$. In addition, the largest invariant set contained in $\mathcal{D}$ such that $\frac{dL}{dt} = 0$ is $\{E_1\}$. If follows from Lasalle's invariance principle [16] that E_1 is globally asymptotically stable in $\mathcal{D}$ when $\mathcal{R}_0 < 1$. Obviously the goal treatment is to eliminate the tumor by infection of cancer cells. Thus making E_1 globally asymptotically stable (GAS) is not useful. So we will avoid $\mathcal{R}_0 < 1$ since the GAS of the infection free equilibrium means the therapy does not have any effect.

3.2 Endemic equilibrium and its stability

When $\mathcal{R}_0 \geq 1$, the condition for the stability of the infection-free equilibrium is violated. It is crucial to prove that the tumor cells will not increase indefinitely. To do so, we calculate the uniform or endemic equilibrium and study its stability.

Let $E^* = (x^*, y^*, v^*, w^*)$ be any endemic equilibrium of the model (1), where $y^* > 0$ and $v^* > 0$. Setting the right hand side of (1) to zero gives after some mathematical manipulations

$y^* = \frac{\beta w_0}{\alpha[\delta(1-u)+\mu]}x^* - \frac{\gamma}{\alpha[\delta(1-u)(b-1)-\mu]} = \frac{r(1-u)x^*}{K[\delta(1-u)+\mu+\frac{r(1-u)}{K}x^*]}(x_0 - x^*)$

$v^* = \frac{\delta(1-u)(b-1)-\mu}{\gamma}y^*$ and $w^* = w_0 = \frac{\eta u p}{\eta u + h}$. Since y^* is non-negative, we have

$x^* > \frac{\gamma[\delta(1-u)+d]}{\beta w_0[\delta(1-u)(b-1)-\mu]}$. Furthermore, we easily demonstrate that $x_0 > x^*$. Hence, we have after simple calculations $\frac{\beta w_0 x_0 b\delta(1-u)}{(\mu+\delta(1-u))(\gamma+\beta w_0 x_0)} > 1$, i.e $\mathcal{R}_0 > 1$. Hence, the uniform equilibrium exist if $\mathcal{R}_0 > 1$. Now, substituting the expressions of y^*, $v^*$and w^*, we finally obtain the following equation in term of x^*:

$$a_2(x^*)^2 + a_1(x^*) + a_0 = 0, \tag{4}$$

where: $a_0 = -\frac{\gamma x_0(\delta(1-u)+\mu)}{\alpha(\delta(1-u)(b-1)-\mu)}$, $a_1 = \frac{\beta w_0 x_0}{\alpha(r(1-u)-\mu)} - x_0 - \frac{\gamma}{\alpha(\delta(1-u)(b-1)-\mu)}$ and $a_2 = 1 + \frac{\beta w_0}{\alpha(r(1-u)-\mu)}$.

It is clear that $a_0 < 0$, $a_2 > 0$ and the sign of a_1 can be positive or negative. Thus, the number of possible real roots of the polynomial (4) depends on the signs of a_1. However, using the center manifold theory, we show that if $\mathcal{R}_0 > 1$, model system (1) has exactly one endemic equilibrium which is locally asymptotically stable. With the help of Theorem 4.1 by Castillo-Chavez and Song in [2], we have the following result.

Proposition 4: *Model system (1) undergoes a unique endemic equilibrium E^* which is locally asymptotically stable for $\mathcal{R}_0 > 1$.*

Proof: In the case when $\mathcal{R}_0 = 1$, one of the eigenvalues of $J(E_1)$ vanishes, so we cannot apply the linearization method. In such case, we can resort to the center manifold theory. If we consider the burst size b as a bifurcation parameter, we can calculate its critical value

$$b = b^* = \frac{(\delta(1-u)+\mu)(\gamma+\beta w_0 x_0)}{\beta\delta(1-u)w_0 x_0} \tag{5}$$

such that $\mathcal{R}_0 < 1$ when $b < b^*$ and $\mathcal{R}_0 > 1$ when $b > b^*$. The Jacobian matrix of the system evaluated at E_1 when $b = b^*$ has a simple zero eigenvalue, and all the other eigenvalues have negative real parts. Therefore, the center manifold theory can be applied to study the dynamics of (1) near $b = b^*$. The right eigenvector and left eigenvector of the Jacobian matrix $J(E_1)$ associated with the zero eigenvalue are given by $W = \Big(-\frac{\beta w_0(r(1-u)x_0+K(\delta(1-u)+\mu))}{r(1-u)(\delta(1-u)+\mu)}w_3, \frac{\beta w_0 x_0}{\delta(1-u)+\mu}, w_3 > 0, 0\Big)^T$ and $V = \Big(0, \frac{\gamma+\beta w_0 x_0}{\beta w_0 x_0}v_3, v_3 > 0, 0\Big)^T$ respectively.

The local stability near the bifurcation parameter $b = b^*$ is determine by the sign of constants $\mathcal{A}$ and $\mathcal{B}$ defined by Theorem 4.1 in [2]. Let $f = (f_1, f_2, f_3, f_4)^T$, where $f(x, y, v, w, b)$ is the function defined by the right-hand side of (1). As $v_1 = v_4 = 0$, the nonvanishing partial derivatives of f at (E_1, b^*) are given by
$\frac{\partial^2 f_2}{\partial x\partial v} = \frac{\partial^2 f_2}{\partial v\partial x} = -\frac{\partial^2 f_3}{\partial x\partial v} = -\frac{\partial^2 f_3}{\partial v\partial x} = \beta w_0, \frac{\partial^2 f_2}{\partial v^2} = -\frac{\partial^2 f_3}{\partial v^2} = -2\alpha\beta w_0 x_0, \frac{\partial^2 f_2}{\partial y\partial b} = \delta(1-u)$.

Therefore, the constant $\mathcal{A}$ is

$$\mathcal{A} = -2\gamma v_3 w_3^2\Big[\alpha + \frac{\beta w_0\big(r(1-u)x_0 + K(\delta(1-u)+\mu)\big)}{r(1-u)(\delta(1-u)+\mu)x_0}\Big] < 0. \tag{6}$$

Furthermore, we have that,

$$\mathcal{B} = v_3 w_2 \frac{\partial^2 f_2}{\partial y \partial b}(E_0, b^*) = \frac{\beta\delta(1-u)w_0 x_0}{\delta(1-u)+\mu} v_3 w_3 > 0. \tag{7}$$

Since $\mathcal{A} < 0$ and $\mathcal{B}$ is always positive, from theorem 4.1 in [2] , we can conclude that E^* is locally asymptotically stable if $\mathcal{R}_0 > 1$. This conclude the proof. ■

Figure (1) shows the bifurcation diagrams of all populations with $\mathcal{R}_0$ as bifurcation parameter. It is clear that the IFE is stable when $\mathcal{R}_0 < 1$ while if $\mathcal{R}_0 > 1$, the IFE is unstable and there exist a unique uniform equilibrium which is stable. Thus, the model system (1) exhibits forward bifurcation at $\mathcal{R}_0 = 1$. Note that, the equilibrium point E^* correspond to the partial success of therapy

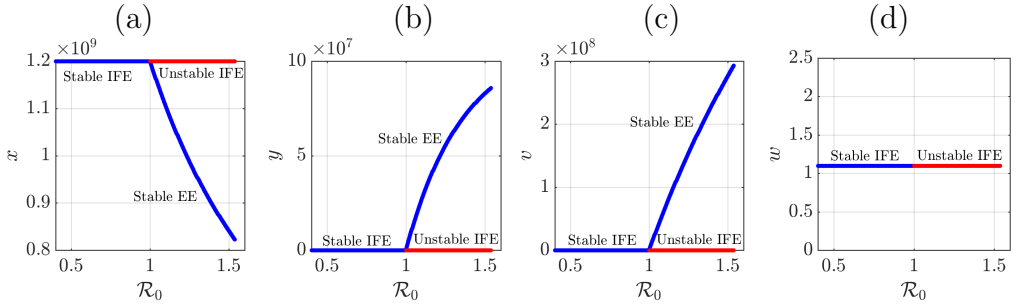

Figure 1: Fixed points bifurcation diagrams of system (1). (a) x, (b) y, (c) v and (d) w. The notations IFE and EE stand for Infection free-equilibrium and endemic equilibrium respectively.

since the presence of oncolytic viruses reduces the number of uninfected glioma cells. The stability of this equilibrium implies a permanent reduction of tumor burden for larger values of basic reproduction ratio $\mathcal{R}_0$, even if the therapy is not completely successful.

3.3 Sensitivity analysis and simulations

3.3.1 Sensitivity analysis of the basic reproduction number

Herein, we appraise the impact of parameters of the model system (1) on the reproduction number $\mathcal{R}_0$. We perform it by computing the elasticity indexes of $\mathcal{R}_0$, with respect to parameter values given in Table 1. According to the approach proposed in [5], the elasticity index of $\mathcal{R}_0$ with respect to a parameter τ, where τ is any of the parameters in Table 1 reflected in the expression of $\mathcal{R}_0$, is given by

$$\mathcal{S}^{\tau}_{\mathcal{R}_0} = \left(\frac{\partial \mathcal{R}_0}{\partial \tau}\right)\left(\frac{\tau}{\mathcal{R}_0}\right). \tag{8}$$

Table 2: Elasticity indexes of the basic reproduction number $\mathcal{R}_0$

Parameter	r	K	η	p	h	β	δ	b	γ	u	μ
Elasticity index	0.66	0.99	0.45	0.99	-0.45	0.99	0.29	1.00	-0.99	-0.50	-0.95

Since these indexes quantify the ratio of relative changes on $\mathcal{R}_0$ in response to corresponding changes in the parameters, they can identify critical parameters for disease control. Table 2 displays the elasticity indexes of $\mathcal{R}_0$ to the parameters of the model. We observe that, the reproduction number is most sensitive to the burst size parameter b with an elasticity index of 1. It is also highly sensitive to the viral clearance γ , and the maximum number of CAR on cell surface, p. Qualitatively, $\mathcal{R}_0$ increases by 10% for an increase in burst size of 10%. $\mathcal{R}_0$ increases (resp. decreases) by 9.9% when p, K and β (resp. γ) increase by 10%.

3.3.2 Impact of combined effects of burst size and MEK inhibitors intensity on the reproduction number

In the previous section, we found that the population of glioma cells can be reduced when the reproduction number $\mathcal{R}_0$ is greater than one. Since b and u are keys parameters characterizing the therapeutic effect of treatment, one may wish to assess their combined influence on the basic reproduction number $\mathcal{R}_0$ with the ultimate aim to control the growth and spread of glioma cells. For $\mathcal{R}_0 \neq 0$, we have $b \neq 0$, $u \neq 0$, and $u \neq u_c = 1 - \mu/r$. Furthermore, $\frac{\partial \mathcal{R}_0}{\partial b} = \dfrac{\beta\delta w_0 x_0(1-u)}{(\delta(1-u)+\mu)(\gamma+\beta w_0 x_0)} > 0$ and $\frac{\partial \mathcal{R}_0}{\partial u} = -\frac{\beta b\delta\mu w_0 x_0}{(\delta(1-u)+\mu)(\gamma+\beta w_0 x_0)} + \frac{\beta b\delta\gamma(1-u) w_0 x_0}{(\delta(1-u)+\mu)(\gamma+\beta w_0 x_0)^2}\left[x_0 \frac{\eta p h}{(\eta u+p)^2} - w_0 \frac{\mu K}{r(1-u)^2}\right]$.

The analysis of this last expression shows that $\frac{\partial \mathcal{R}_0}{\partial u}$ can be positive or negative depending of the value of u. Hence, we can conclude that the burst size always has a positive impacts on glioma control by increasing the reproduction number $\mathcal{R}_0$. But the intensity of MEK inhibitors considered either solely or combined can have a positive or negative impact on the disease control. This important result is illustrated in Fig.2. Figure 2(a) shows the range value of inhibitors intensity required to reduce the tumor load when the burst size is fixed. The other parameters are given in table 1. We see that regardless on the value of u, there is a minimal value of b for which $\mathcal{R}_0$ is greater than 1. Furthermore, the minimum (resp. maximum) value of u required to bring $\mathcal{R}_0$ above 1 decreases (resp. increases) when b increases. Fig. 2(b) highlights that, if the burst size is below about 200, irrespective of the value of the intensity of MEK inhibitors, $\mathcal{R}_0$ will never be brought above 1, and consequently, glioma can never be controlled. Fig.2(c) is the bifurcation diagram (contour plot) of $\mathcal{R}_0$ in the $(u-b)$ space by combining the plots in Fig.2(a) and (b). It highlights

that, if intensity of MEK inhibitor u is between 0.2 and 0.6, reproduction ratio will remain greater than 1 whenever $b > 200$. Therefore, any couple (b, u) which is in the set $]0; 1000] \times [0; 0.8]$ can be suitably chosen such that $\mathcal{R}_0$ is greater than 1 (that is, glioma is reduced).

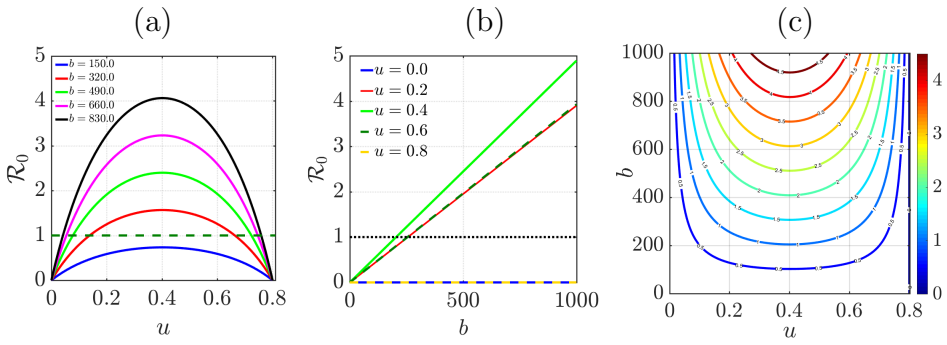

Figure 2: Basic reproduction number, $\mathcal{R}_0$ versus: (a) the MEK inhibitor intensity for different b; (b) burst size for different value of u; (c) u and b (Contour plot). Other parameters are given in Table 1.

3.4 Existence of Hopf bifurcation

A Hopf bifurcation refers to the phenomenon from which steady states lose their stability and give rise to periodic solutions, as a control parameter crosses its critical values. Since the infection-free equilibrium E_1 lies on the boundary of the invariant region $\mathcal{D}$, it is clear that there cannot exist a closed orbit surrounding E_1. Thus, we will only consider the existence of Hopf bifurcation around an endemic equilibrium E^*. We choose the burst size b as the bifurcation parameter. From the Jacobian matrix of the system at E^*, its local stability is completely determined by the one of the matrix:

$$J^* = \begin{pmatrix} \frac{-r(1-u)x^*}{K} & \frac{-r(1-u)x^*}{K} & \frac{-\beta m x^*}{(1+\alpha v^*)^2} \\ \frac{\beta m v^*}{1+\alpha v^*} & -\delta(1-u) - \mu & \frac{\beta m x^*}{(1+\alpha v^*)^2} \\ \frac{-\beta m v^*}{1+\alpha v^*} & b\delta(1-u) & \frac{-\beta m x^*}{(1+\alpha v^*)^2} - \gamma \end{pmatrix}$$

The characteristic equation of J^* is

$$\lambda^3 + \tilde{a}_2\lambda^2 + \tilde{a}_1\lambda + \tilde{a}_0 = 0, \tag{9}$$

where $\tilde{a}_2 = \frac{r(1-u)(1+\alpha v^*)^2 + (\delta(1-u)+\gamma+\mu)AK(1+\alpha v^*) + K\beta w_0}{AK(1+\alpha v^*)}$,

$\tilde{a}_1 = \frac{1}{KA^2(1+\alpha v^*)}\Big([rA(1-u)(\delta(1-u)+\gamma+\mu) + r\beta w_0(1-u)](1+\alpha v^*)^2 + \Big[K\gamma(\delta(1-u)+\mu)A^2 + r\beta w_0(1-u)\Big](1+\alpha v^*) + K\beta w_0(\delta(1-u)(b-1)-\mu)A - K\beta^2 w_0^2\Big)$,

$\tilde{a}_0 = \frac{1}{KA^2(1+\alpha v^*)}\Big(r\gamma(1-u)[(\delta(1-u)+\mu)A + \beta w_0](1+\alpha v^*)^2 + r\beta w_0(1-u)(\delta(1-$

$u)(b-1)-\mu)(1+\alpha v^*)+K\beta^2 w_0^2(\delta(1-u)(b-1)-\mu)\Big)$, with $A=\frac{\delta(1-u)(b-1)-\mu}{\gamma[\delta(1-u)+\mu]}\beta w_0$. As b is the bifurcation parameter, b_c represents its associated critical value. Let Q be a real valued continuously differentiable function defined by $Q=\tilde{a}_1\tilde{a}_2-\tilde{a}_0$. At $b=b_c$, we have $Q(b_c)=0$, and the characteristic equation can be written as

$$(\lambda^2+\tilde{a}_1)(\lambda+\tilde{a}_2)=0.$$

This equation has three roots namely $\lambda_i (i=1,2,3)$, where $\lambda_{1,2}=i\psi_0$, $\psi_0=\sqrt{\tilde{a}_1}$ are purely imaginary, and $\lambda_3=-\tilde{a}_2$ is real; for $\tilde{a}_2>0$, $\lambda_3<0$.
Let us consider that, $\lambda_{1,2}=\phi(b)+i\psi(b)$. Substituting this into the characteristic equation and separating the real and the imaginary parts, we get

$$\begin{aligned}\phi^3-3\phi\psi^2+\tilde{a}_2(\phi^2-\psi^2)+\tilde{a}_1\phi+\tilde{a}_0=0,\\ 3\phi^3\psi-\psi^3+2\tilde{a}_2\phi\psi+\tilde{a}_1\psi=0.\end{aligned}\tag{10}$$

Differentiating both equations of (10), we obtain

$$\begin{aligned}M_1(b)\frac{\partial\phi(b)}{\partial b}-M_2(b)\frac{\partial\psi(b)}{\partial b}+M_3=0,\\ M_2(b)\frac{\partial\phi(b)}{\partial b}+M_1(b)\frac{\partial\psi(b)}{\partial b}+M_4=0,\end{aligned}\tag{11}$$

where $M_1(b)=3\phi^2+2\tilde{a}_2\phi-3\psi^2+\tilde{a}_1, M_2(b)=6\phi\psi+2\tilde{a}_2\psi, M_3(b)=(\phi^2-\psi^2)\frac{\partial\tilde{a}_2(b)}{\partial b}+\phi\frac{\partial\tilde{a}_1(b)}{\partial b}+\frac{\partial\tilde{a}_0(b)}{\partial b}, M_4(b)=2\phi\psi\frac{\partial\tilde{a}_2(b)}{\partial b}+\psi\frac{\partial\tilde{a}_1(b)}{\partial b}$. For $b=b_c$, we have $M_1(b)=-2\tilde{a}_1, M_2(b)=2\tilde{a}_2\sqrt{\tilde{a}_1}, M_3(b)=-\tilde{a}_1\frac{\partial\tilde{a}_2(b)}{\partial b}+\frac{\partial\tilde{a}_0(b)}{\partial b}, M_4(b)=\sqrt{\tilde{a}_1}\frac{\partial\tilde{a}_1(b)}{\partial b}$. We solve (11) as a function of $\frac{\partial\phi(b)}{\partial b}$ and get

$$\frac{\partial\phi(b)}{\partial b}=\frac{M_1M_3+M_2M_4}{M_1^2+M_2^2}.\tag{12}$$

If $\frac{\partial\phi(b)}{\partial b}\neq 0$, the transversality condition holds which means that the eigenvalues cross the imaginary axis and hence Hopf bifurcation can occurs at $b=b_c$.

The biological implication of the existence of Hopf bifurcation is that, the disease will come back after a time corresponding to the period of bifurcating solutions even if it had disappeared. This situation have to be avoided during therapy. To illustrate the above theoretical results on the Hopf bifurcation, numerical computations are done. For the values of $p=8$, $\gamma=0.65$ and for other parameters values given in Table 1, we obtain the critical values of burst size $b_c=1.399889393, b_c=2.130016794$ and $b_c=28.81030802$ at which E^* changes its stability. We choose the third value since the first and the second one are not biologically sufficient for our analysis. Figures 3a and 3b show the solution of uninfected glioma cells, for $b=10(<b_c)$ and $b=50(>b_c)$, respectively. From these figures, it is inferred that for $b<b_c$, all the population attain his equilibrium value and for $b>b_c$, periodic oscillations arise after Hopf

bifurcation. As conclusions, tumors can oscillate spontaneously or in response to the applied therapy. It can then rebound after some period depending on its severity. This behavior is known as Jeff's phenomenon [24] and is widely found in clinical cases.

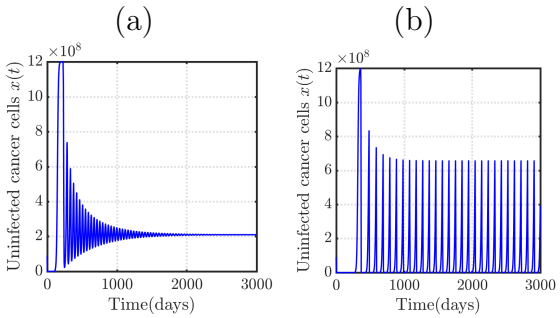

Figure 3: Temporal solution of (a) $x(t)$ for $b = 10 < b_c$ which shows that E^* is stable , (b) $x(t)$ for $b = 50 > b_c$ which shows that E^* is unstable.

4 Application of optimal control to the model

4.1 Controlled model derivation and optimal problem setting

In order to alleviate the pain of patients and extend their living time, we will investigate how assigned an optimal treatment policy over a finite time period $[0, T_f]$ sketched an effective treatment protocol. The main of this part is to analyse how to give an optimal treatment where MEK inhibitors and oncolytic adenoviruses might be an efficient tools to assist the patient fight against cancer in general with a particularity given to glioma. To follow this aims, we set the control variables $u_1(t)$ and $u_2(t)$ to respectively be the supply of MEK inhibitors and adenovirus injected into the model systems equations (1) to obtain the following control equations:

$$\begin{cases} \dot{x} = r(1-u_1(t))x(1-\frac{x+y}{K}) - \frac{\beta w x v}{1+\alpha v} - \mu x, \\ \dot{y} = \frac{\beta w x v}{1+\alpha v} - \delta(1-u_1(t))y - \mu y, \\ \dot{v} = b\delta(1-u_1(t))y - \frac{\beta w x v}{1+\alpha v} - \gamma v + u_2(t), \\ \dot{w} = \eta u_1(t)(p-w) - hw. \end{cases} \tag{13}$$

Recall that the objective of the control is to minimize the total tumor cells (i.e $(x + y)$) at the end of treatment period, while keeping the cost of the control as low as possible. To achieve this goal, we incorporate the relative costs associate with each control or combination of policies directed towards

controlling the spread of cancer cells. The objective function can then be defined as:

$$\mathcal{J}(u_1, u_2) = \int_0^{T_f} \big[x(t) + y(t) + \frac{\sigma_1}{2}u_1(t)^2 + \frac{\sigma_2}{2}u_2(t)^2\big]dt, \tag{14}$$

where the control set is

$$\mathbb{U} = \big\{(u_1, u_2) : 0 \leq u_i \leq u_i^{\text{MTD}} \text{ for } t \in [0, T_f], i = 1, 2\big\},$$

where T_f represents a given therapeutic period, subject to the system of differential Eq.(13), with initial conditions $x(0) \geq 0$, $y(0) \geq 0$, $x(0) \geq 0$, $x(0) \geq 0$ and $u_i(0) \geq 0, i = 1, 2$. The constants σ_1 , σ_2 which are positive, represent the weight factors on control indicating the cost of drugs and also exhibit a measure of the toxicity of drugs in our body. Moreover, σ_1 and σ_2 play crucial role for balancing the size terms and the square of the controllers u_1^2, u_2^2, are taken to remove some unwanted side effects of drugs, as well as to consider their overdoses [10, 12]. They also explain the high toxicity for our body during drug administration. It is not difficult to prove that there exists an optimal control pair $(u_1^*(t), u_2^*(t))$ and a corresponding solution $(x^*; y^*; v^*; w^*)$ of the initial value problem (13) that minimizes the cost function $\mathcal{J}$ in $\mathbb{U}$ such that

$$\mathcal{J}(u_1^*, u_2^*) = min\{\mathcal{J}(u_1, u_2) : (u_1, u_2) \in \mathbb{U}\}. \tag{15}$$

4.2 Characterization of an optimal control

The necessary conditions that an optimal control must satisfy come from the Pontryagin's Maximum Principle (PMP) [20]. In order to seek for the minimal value of the Lagrangian defined by
$\mathcal{L}(x, y, u_1, u_2) = x + y + \frac{\sigma_1}{2}u_1^2 + \frac{\sigma_1}{2}u_2^2$,
we define the Hamiltonian $\mathcal{H}$ for the control problem as

$$\begin{aligned}
\mathcal{H} &= \mathcal{L} + \zeta_1\frac{dx}{dt} + \zeta_2\frac{dy}{dt} + \zeta_3\frac{dv}{dt}\zeta_4\frac{dw}{dt} \\
&= x + y + \frac{\sigma_1}{2}u_1^2 + \frac{\sigma_2}{2}u_2^2 + \zeta_1\Big[r(1-u_1)x(1-\frac{x+y}{K}) - \frac{\beta wxv}{1+\alpha v} - \mu x\Big] \\
&+ \zeta_2\Big[\frac{\beta wxv}{1+\alpha v} - \delta(1-u_1)y - \mu y\Big] + \zeta_3\Big[b\delta(1-u_1)y - \frac{\beta wxv}{1+\alpha v} - \gamma v + u_2\Big] \\
&+ \zeta_4\Big[\eta u_1(p-w) - hw\Big],
\end{aligned} \tag{16}$$

where $\zeta_i = (\zeta_1, \zeta_2, \zeta_3, \zeta_4)$ are called the adjoint variables or the co-state variables for x, y, v, w. With the help of Pontryagin's Maximum Principle, we obtained a minimized Hamiltonian that reduces the objective function to its lower value. This allows the characterization of the optimal control pair (u_1^*, u_2^*) in the following result:

Theorem 5: *Given optimal control variables* $(u_1^*, u_2^*) \in \mathbb{U}$ *and* $(x^*; y^*; v^*; w^*)$ *are corresponding optimal state variables of the control system (13). Then there exists the adjoint variables* $\zeta_i, i = 1, 2, 3, 4$ *that satisfies the following equations.*

$$\begin{aligned}
\dot{\zeta_1} = & -1 - \zeta_1\Big[r(1-u_1)\Big(1-\frac{2x+y}{K}\Big) - \frac{\beta w v}{1+\alpha v} - \mu\Big] - \zeta_2\Big[\frac{\beta w v}{1+\alpha v}\Big] + \zeta_3\Big[\frac{\beta w v}{1+\alpha v}\Big],\\
\dot{\zeta_2} = & -1 + \zeta_1\Big[\frac{r(1-u_1)x}{K}\Big] + \zeta_2\Big[\delta(1-u_1) + \mu\Big] - \zeta_3 b\delta(1-u_1),\\
\dot{\zeta_3} = & \ \zeta_1\Big[\frac{\beta w x}{(1+\alpha v)^2}\Big] - \zeta_2\Big[\frac{\beta w x}{(1+\alpha v)^2}\Big] + \zeta_3\Big[\frac{\beta w v}{(1+\alpha v)^2} + \gamma\Big],\\
\dot{\zeta_4} = & \ \zeta_1\frac{\beta x v}{1+\alpha v} - \zeta_2\frac{\beta x v}{1+\alpha v} + \zeta_3\frac{\beta x v}{1+\alpha v} + \zeta_4(\eta u_1 + h),
\end{aligned} \tag{17}$$

and transversality conditions

$$\dot{\zeta_i}(T_f) = 0, i = 1, 2, 3, 4. \tag{18}$$

Furthermore, The corresponding optimal controls (u_1^* *and* u_2^*) *are given as,*

$$\begin{aligned}
u_1^* = & min\Big\{u_1^{MTD}, max(0, \frac{m}{\sigma_1})\Big\},\\
u_2^* = & min\Big\{u_2^{MTD}, max(0, \frac{\zeta_3}{\sigma_2})\Big\},
\end{aligned} \tag{19}$$

where $m = \Big[\zeta_1 r x^*\Big(1-\frac{x^*+y^*}{K}\Big) - \zeta_2\delta y^* + \zeta_3 b\delta y^* - \zeta_4\eta(p-w^*)\Big]$, *and* $\zeta_i (i = 1, 2, 3, 4)$ *the solutions of (17).*

Proof. Let u_1^* and u_2^* be the given optimal control functions and $(x^*; y^*; v^*; w^*)$ be the corresponding optimal state variables of the system (13) that minimize the cost or objective functional (14). Then by Pontryagin's maximum principle [20], the differential equations governing the adjoint variables are obtained by differentiation of the Hamiltonian function, evaluated at the optimal states. Then we can write

$$\dot{\zeta_1} = -\frac{\partial \mathcal{H}}{\partial x}, \dot{\zeta_2} = -\frac{\partial \mathcal{H}}{\partial y}, \dot{\zeta_3} = -\frac{\partial \mathcal{H}}{\partial v}, \dot{\zeta_4} = -\frac{\partial \mathcal{H}}{\partial w}, \tag{20}$$

with zero time condition (transversality). To get the characterization of the optimal control, we solve the interior equation of its corresponding set obtained by differentiating the Hamiltonian function with respect to the controllers. We obtain: $\frac{\partial \mathcal{H}}{\partial u_1} = 0, \frac{\partial \mathcal{H}}{\partial u_2} = 0$, which conduct,using the compact notation to the following choice of the controller bounds:

$u_1^* = \min\Big\{u_1^{\text{MTD}}, \max(0, \frac{m}{\sigma_1})\Big\}$ and $u_2^* = \min\Big\{u_2^{\text{MTD}}, \max(0, \frac{\zeta_3}{\sigma_2})\Big\}$,
with $m = \Big[\zeta_1 rx\Big(1 - \frac{x^*+y^*}{K}\Big) - \zeta_2\delta y^* + \zeta_3 b\delta y^* - \zeta_4\eta(p - w^*)\Big]$. ■

It can be mentioned that the optimal controllers and states are found by solving the optimal system, which consists of the state system (13), the adjoint system (17), initial conditions, transversality conditions (18) and the characterization of the optimal control (19). In addition, the second derivative of the Lagrangian with respect to u_1 and u_2 are positive, which shows that the optimal problem is minimum at u_1^* and u_2^* .

4.3 Numerical results and biological implications

We use parameter values of table 1 in this section to prove numerically the optimal plan for performing treatment. We consider for these purposes a period of $T_f = 30$ days with $\sigma_1 = 1, \sigma_2 = 0.001$ and initial conditions of $(x(0), y(0), v(0), w(0)) = (4.2 \times 10^7; 0.0; 1 \times 10^8; 2 \times 10^3)$. The control bounds are chosen as $u_1^{MTD} = 0.5$ and $u_2^{MTD} = 100$. Moreover, we use a forward-backward fourth-order Runge-Kutta method [15] to present adopted treatment strategy ie results when both controllers are considered.

Fig.4 shows the dynamics of the optimality system when combined therapy is considered. We find that $x(T_f) = 1.498 \times 10^6$, $y(T_f) = 3.591 \times 10^4$, $v(T_f) = 1.511 \times 10^5$ and $w(T_f) = 2.835$. It is seen that, the uninfected cancer cells retrench after a treatment period of 30 days (Fig.4a), but seems to rebound to a lower value compared to the initial size. As expected, the population of glioma cells with control is more sharply decreased than the population without any control. Alike observations are made for the infected cancer cells, free virus particles and average level of CAR molecules respectively (Fig.4b-d). We see that, the number of infected cells and virus particles is very small without control and they increase rapidly while the uninfected cells rapidly decrease, at first, due to supply of viruses, but then slowly disappear when the treatment ends. Furthermore, from Fig.4e and f, we observe that the control u_1 starts to be active after 7 days (one week) before falling to zero after 30 days. u_2 remains constant upto 2 days and falls to zero after 30 days also. On the other hand, one can say that the release rate of MEK is zero when $t \in [0, 7]$, rise after to the maximal dose, and vanishes at the end of control($T_f = 30$). The right panel represents the profile of $u_2(t)$ illustrating that, at the beginning of the therapeutic process the number of virus particles is maximal and decreases from 100 to about 35 that is 65% after two days. This means that, at the early stage of treatment, we need only viruses and after one week, MEK inhibitors will be supply at its maximal dose. These observations shows that, the MEK inhibitors based therapy is needed to keep the level of infected cancer cells and uninfected cancer cells down and unfortunately to resist cancer recurrence.

Furthermore, based on patients' different factors, therapeutic strategies must be taken into account such that the size of effects due to viruses and drug administration are minimized.

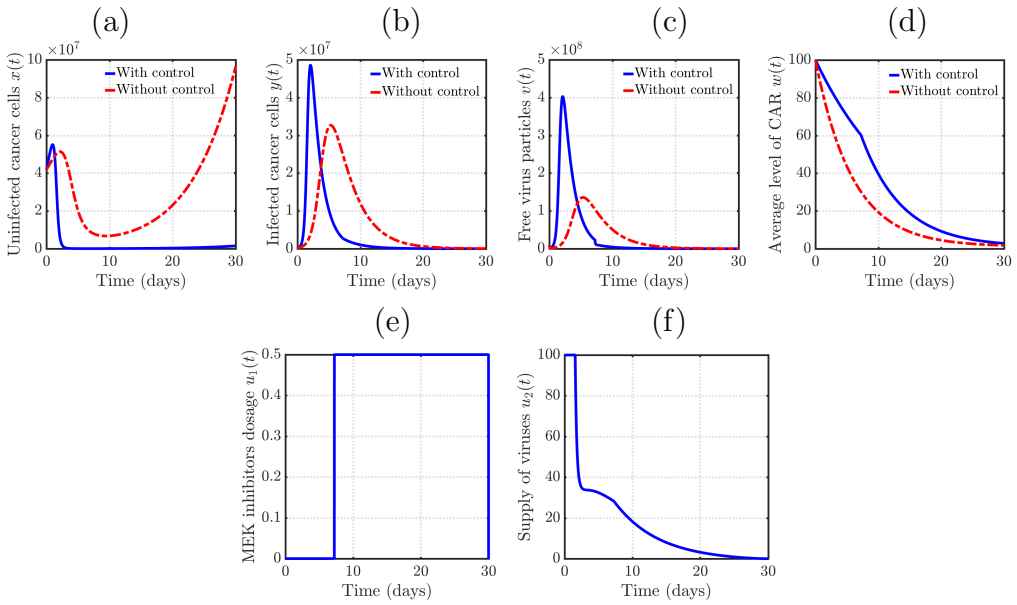

Figure 4: Variation of the state variables in the presence and in the absence of control (b=400); (a) $x(t)$, (b) $y(t)$, (c) $v(t)$, and (d) $w(t)$.Variation of Optimal control (e) $u_1(t)$ and (f) $u_2(t)$.

5 Conclusion

In this paper, a nonlinear mathematical model is analyzed for the control of brain tumor by regulating the growth of cancer cells by combination therapies, using CRAds in conjunction with MEK inhibitors. It is assumed that the growth rate of glioma cells follows a logistic one. We presented the theoretical study of the proposed model, the calculation and the sensitivity analysis of the basic reproduction number and finally the optimal control of the model through two therapies and their combination. This helps us to obtain some results clinically observed and to have an idea on the therapeutic protocol to be used. However, various factors like immune effectors, random noise, environmental disturbances (supply of oxygen and nutrients, immunological state of the host, exposure to chemical agents and electromagnetic radiations...) [14], together with the food habit are not incorporated in the proposed model. Treatment of these questions with such cases remain and are under investigation.

References

[1] Camara B. I., Mokrani H., Afenya E., Mathematical modeling of gliomas therapy using oncolytic viruses, *Mathematical Biosciences,* **10** (3) (2013), 565-578. https://doi.org/10.3934/mbe.2013.10.565

[2] Castillo-Chavez C., Song B., Dynamical models of tuberculosis and their applications, *Mathematical Biosciences and Engineering,* **1** (2) (2004), 361-404. https://doi.org/10.3934/mbe.2004.1.361

[3] Chang S. M., Parney I. F., Huang W., Anderson F. A., Asher A. L., Bernstein M., Lillehei K. O., Brem H., Berger M. S., Laws E. R., Patterns of Care for Adults With Newly Diagnosed Malignant Glioma, *JAMA,* **293** (2005), 557. https://doi.org/10.1001/jama.293.5.557

[4] Chiocca E. A., Abbed K. M., Tatter S., Louis D. N., Hochberg F. H., Barker F., A phase I open-label, dose-escalation, multi-institutional trial of injection with an E1B-Attenuated adenovirus, ONYX-015, into the peritumoral region of recurrent malignant gliomas, in the adjuvant setting, *Mol. Ther.,* **10** (5) (2004), 958-966. https://doi.org/10.1016/j.ymthe.2004.07.021

[5] Chitnis N., Hyman J. M., Cushing J. M., Determining important parameters in the spread of malaria through the sensitivity analysis of a mathematical model, *Bulletin of Mathematical Biology,* **70** (2008), 1272-1296. https://doi.org/10.1007/s11538-008-9299-0

[6] El-alami laaroussi A., El hia M., Rachik M., Benlahmar E., Rachik Z., Analysis of a Mathematical Model for Treatment of Cancer with Oncolytic Virotherapy, *Applied Mathematical Sciences,* **8** (19) (2014), 929-940. https://doi.org/10.12988/ams.2014.311663

[7] Elzbieta R., Urszula L., Heinz S., Optimal Control for a Mathematical Model of Glioma Treatment with Oncolytic Therapy and TNF-α Inhibitors, *Journal of Optimal Theory Applied,* **176** (2018), 456-477. https://doi.org/10.1007/s10957-018-1218-4

[8] Friedman A., Tian J. P., Fulci G., Chiocca E. A., Wang J., Glioma virotherapy: The effects of innate immune suppression and increased viral replication capacity, *Cancer Research,* **66** (2006), 2314-2319. https://doi.org/10.1158/0008-5472.can-05-2661

[9] Jianjun P. T., The replicability of oncolytic virus: defining conditions in tumor virotherapy, *Mathematical Biosciences and Engineering,* **8** (3) (2011), 841-860. https://doi.org/10.3934/mbe.2011.8.841

[10] Kar, T. K., Batabyal A, Stability analysis and optimal control of a sir epidemic model with vaccination, *Biosystems,* **104** (2011), 127-135. https://doi.org/10.1016/j.biosystems.2011.02.001

[11] Kim M., Sumerel L. A., Belousova N., Lyons G. R., Carey D. E., Krasnykh V., The coxsackievirus and adenovirus receptor acts as a tumour suppressor in malignant glioma cells, *Br. J. Cancer,* **88** (9) (2003), 1411-1416. https://doi.org/10.1038/sj.bjc.6600932

[12] Kusum L., Mishra S. N., Misra A. K., An optimal control problem for carrier dependent doseases, *BioSystems,* **187** (2020), 1-10. https://doi.org/10.1016/j.biosystems.2019.104039

[13] Lasalle J. P., *The The stability of dynamical systems, Regional conference series in applied Mathemetics,* SIAM, Philadelphia, 1976.

[14] Lefever R., Horsthemke W., Bistability in fluctuating environments, *Implications in tumor immunology Bulletin of Mathematical Biology,* **41** (1979), 469-490. https://doi.org/10.1016/s0092-8240(79)80003-8

[15] Lenhart S., Workman J. T., *Optimal Control Applied to Biological Models,* Chapman & Hall/CRC: Boca Raton, FL, USA, 2007. https://doi.org/10.1201/9781420011418

[16] Linsenmann T., Jawork A., Westermaier T., Homola G., Monoranu C. M., Vince G. H., Tumor growth under rhGM-CSF application in an orthotopic rodent glioma model, *Oncolytic Letter,* **17** (6) (2019), 4843-4850. https://doi.org/10.3892/ol.2019.10179

[17] Malinzi J., Rachid O., Amina E., Delfim F. M. T., Jane W. K. A., Enhancement of chemotherapy using oncolytic virotherapy: mathematical and optimal control analysis, *Mathematical Biosciences,* **15** (6) (2018), 1435-1463. https://doi.org/10.3934/mbe.2018066

[18] Monika J., Piotrowska M. B., Jan P., Urszula F., Mathematical modelling of immune reaction against gliomas: Sensitivity analysis and influence of delays, *Nonlinear Analysis: Real World Applications,* **14** (2013), 1601-1620. https://doi.org/10.1016/j.nonrwa.2012.10.020

[19] Okamoto K. W., Priyanga A. I., Petty T. D., Modeling oncolytic virotherapy:Is complete tumor-tropism too much of a good thing?, *Journal of Theoretical Biology,* **358** (2014), 166-178. https://doi.org/10.1016/j.jtbi.2014.04.030

[20] Pontryagin L. S., *Mathematical Theory of Optimal Processes,* CRC Press: Boca Raton, FL, USA, 1987.

[21] Storey K. M., Lawler S. E., Jackson T. L., Modeling Oncolytic Viral Therapy, Immune Checkpoint Inhibition, and the Complex Dynamics of Innate and Adaptive Immunity in Glioblastoma Treatment, *Frontier in Physiology,* **11** (2020). https://doi.org/10.3389/fphys.2020.00151

[22] Stupp R., Mason W. P., Van Den Bent M. J., Weller M., Fisher B., Taphoorn M. J., Belanger K., Brandes A. A., Marosi C., Bogdahn U., Radiotherapy plus concomitant and adjuvant temozolomide for glioblastoma, *New England Journal of Medicine,* **352** (10) (2005), 987-996. https://doi.org/10.1056/nejmoa043330

[23] Suvobroto N., Maciej S. L., Adenoviral virotherapy for malignant brain tumors, *Expert Opin. Biol. Ther.,* **9** (6) (2009), 737-747. https://doi.org/10.1517/14712590902988451

[24] Thomlinson R., Measurement and management of carcinoma of the breast, *Clin. Radiol.,* **182** (1982), 481-493. https://doi.org/10.1016/s0009-9260(82)80153-0

[25] Turnell A. S., Grand R. J., Gallimore P. H., The replicative capacities of large E1B-null group A and group C adenoviruses are independent of host cell p53 status, *Journal of Virology,* **73** (3) (1999), 2074-2083. https://doi.org/10.1128/jvi.73.3.2074-2083.1999

[26] Ulasov I. V., Borovjagin A. V., Schroeder B. A., Baryshnikov A. Y., Oncolytic adenoviruses: A thorny path to glioma cure, *Genes & Diseases***1** (2014), 214-226. https://doi.org/10.1016/j.gendis.2014.09.009

[27] Van de Driessche P., Watmough, J., Reproduction numbers and Subthreshold endemic equilibria for compartmental models of disease transmission, *Mathematical Biosciences,* **180** (2002), 29-48. https://doi.org/10.1016/s0025-5564(02)00108-6

[28] Wollmann G., Ozduman K., van den Pol A. N., Oncolytic virus therapy for glioblastoma multiforme: concepts and candidates, *Cancer Journal,* **18** (1) (2012), 69-81. https://doi.org/10.1097/ppo.0b013e31824671c9

[29] Zurakowski R.,Wodarz D., Model-driven approaches for in vitro combination therapy using ONYX-015 replicating oncolytic adenovirus, *Journal of Theoretical Biology,* **245** (2007), 1-8. https://doi.org/10.1016/j.jtbi.2006.09.029

Received: September 25, 2020; Published: October 18, 2020